

Contextualized Keyword Representations for Multi-modal Retinal Image Captioning

Jia-Hong Huang

University of Amsterdam, Netherlands
j.huang@uva.nl

Ting-Wei Wu

Georgia Institute of Technology, USA
waynewu@gatech.edu

Marcel Worring

University of Amsterdam, Netherlands
m.worring@uva.nl

ABSTRACT

Medical image captioning automatically generates a medical description to describe the content of a given medical image. A traditional medical image captioning model creates a medical description only based on a single medical image input. Hence, an abstract medical description or concept is hard to be generated based on the traditional approach. Such a method limits the effectiveness of medical image captioning. Multi-modal medical image captioning is one of the approaches utilized to address this problem. In multi-modal medical image captioning, textual input, e.g., expert-defined keywords, is considered as one of the main drivers of medical description generation. Thus, encoding the textual input and the medical image effectively are both important for the task of multi-modal medical image captioning. In this work, a new end-to-end deep multi-modal medical image captioning model is proposed. Contextualized keyword representations, textual feature reinforcement, and masked self-attention are used to develop the proposed approach. Based on the evaluation of the existing multi-modal medical image captioning dataset, experimental results show that the proposed model is effective with the increase of +53.2% in BLEU-avg and +18.6% in CIDEr, compared with the state-of-the-art method. <https://github.com/Jhuangkay/Contextualized-Keyword-Representations-for-Multi-modal-Retinal-Image-Captioning>.

Keyword-Representations-for-Multi-modal-Retinal-Image-Captioning.

KEYWORDS

Multi-modal Medical Image Captioning, Contextualized Word Representations, Retinal Images

ACM Reference Format:

Jia-Hong Huang, Ting-Wei Wu, and Marcel Worring. 2021. Contextualized Keyword Representations for Multi-modal Retinal Image Captioning. In *Proceedings of the 2021 International Conference on Multimedia Retrieval (ICMR '21)*, August 21–24, 2021, Taipei, Taiwan. ACM, New York, NY, USA, 8 pages. <https://doi.org/10.1145/nnnnnnn.nnnnnnn>

1 INTRODUCTION

Medical image captioning automatically generates a medical report/description that describes the content of a given medical image [26, 27, 31, 34]. However, traditional medical image captioning methods, e.g., [27, 31, 34], generate a medical description based on given image information only. It is hard to derive abstract medical

Permission to make digital or hard copies of all or part of this work for personal or classroom use is granted without fee provided that copies are not made or distributed for profit or commercial advantage and that copies bear this notice and the full citation on the first page. Copyrights for components of this work owned by others than the author(s) must be honored. Abstracting with credit is permitted. To copy otherwise, or republish, to post on servers or to redistribute to lists, requires prior specific permission and/or a fee. Request permissions from permissions@acm.org.

ICMR '21, August 21–24, 2021, Taipei, Taiwan

© 2021 Copyright held by the owner/author(s). Publication rights licensed to ACM.

ACM ISBN 978-x-xxxx-xxxx-x/YY/MM. . \$15.00

<https://doi.org/10.1145/nnnnnnn.nnnnnnn>

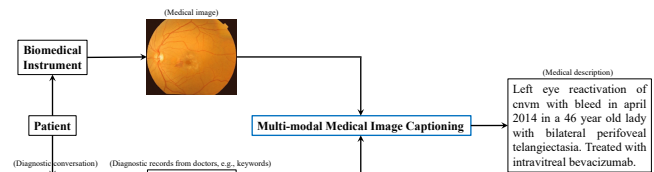


Figure 1: Multi-modal medical image captioning. A multi-modal medical image captioning algorithm takes a medical image, e.g., a retinal image, and text-based diagnostic records, e.g., a set of keywords, as inputs to generate a medical description. The effectiveness of traditional medical image captioning models is improved by the additional input keywords.

descriptions/concepts [27, 31] based on the traditional approaches. Hence, they reduce the effectiveness of medical image captioning.

Multi-modal medical image captioning has been proposed as an approach to make conventional medical image captioning more effective [26]. The main idea of multi-modal medical image captioning is to generate descriptions for a given medical image based on the additional text-based information provided by the doctor, e.g., using keywords to help the medical description generation, visualized in Figure 1. According to [26], keywords commonly exist and they are from the doctors' textual diagnosis records in the early diagnosis process. Traditional medical image captioning only has one input modality, i.e., image, while an efficient choice for multi-modal medical image captioning is a set of keywords, in addition to medical image [26]. Since the set of keywords is considered as one of the main inputs of multi-modal medical image captioning [26], effectively embedding the keywords is important. In [26], the Bag of Words (BoW) approach is used to encode the keywords input for multi-modal medical image captioning. BoW has been used with great success on many natural language processing (NLP) tasks, e.g., language modeling and document classification, but the authors of [52, 55] point out that BoW suffers from the following. First, from the time and space complexity perspective, sparse representations are harder to model by BoW, so the vocabulary requires careful design. If the information in a large representation space is sparse, BoW models are not effective enough. Second, the semantic meaning likely cannot be captured effectively.

In this work, a new approach is proposed that tackles the aforementioned issue to improve the performance of a multi-modal medical image captioning model. According to [9], the commonly used method of static word embeddings, e.g., global vectors for word representation (GloVe) [47] or skip-gram with negative sampling (SGNS) [42], is a better choice to encode the textual input than BoW. However, a limitation with static word embeddings is that all senses of a polysemous word must share a single vector because GloVe and SGNS generate a single representation for each word [9]. As stated

in [9] the approach of contextualized word representations, e.g., Generative Pretrained Transformer-2 (GPT-2), is more effective than static word embeddings. For encoding textual input, the proposed method exploits the contextualized word representations approach, i.e., GPT-2, to more effectively encode input keywords. For visual feature extraction, a pre-trained convolutional neural network (CNN), e.g., VGG16 or VGG19 pre-trained on ImageNet [51, 53], is applied to effectively encode input medical image. Note that experiments conducted in this paper are based on the existing multi-modal retinal image captioning dataset which is proposed by [26]. Retinal images from [26]’s dataset are mostly colorful. Hence, using a CNN pre-trained on ImageNet is helpful in the experiments in terms of low-level features, e.g., color [26]. According to the experimental results, the proposed multi-modal medical image captioning method generates a more accurate and meaningful description for a given retinal image than baselines.

Contributions.

- A new end-to-end deep model for multi-modal medical image captioning is proposed, based on the contextualized keyword representation, textual feature reinforcement module, and masked self-attention mechanism.
- The proposed method is thoroughly validated through experiments on the existing multi-modal retinal image captioning dataset. The experimental results show that the proposed model is more effective than the method based on static word embedding or BoW. The model performance is increased in terms of BLEU and CIDEr.

The rest of this paper is organized as follows: In Section 2, the related work is reviewed. Then, the proposed approach is introduced in Section 3. Finally, an evaluation of the effectiveness of the proposed model is conducted in Section 4, followed by an analysis of the experimental results.

2 RELATED WORK

In this section, the related works, i.e., image captioning, multi-modal medical image captioning, methods of word embeddings, and retinal image dataset are reviewed.

2.1 Image Captioning

The goal of conventional image captioning is to automatically generate a text-based description for a given natural image [10, 28, 60]. In [60], an image captioning model with an encoder-decoder architecture was introduced. A CNN model was considered as an encoder to extract image features. A recurrent neural network (RNN) was considered as a decoder to produce a description for a given natural image, based on the extracted image feature. In [10], a language model was exploited to combine a set of possible words, related to several parts of an input image, and generate a description of the image. The authors of [28] have introduced an approach that embeds language and visual information into a common space. In [14], the authors have proposed a method that focuses on discriminating properties of the visible object. The proposed approach jointly predicts a class label and is used to explain why the predicted label is proper for a given input image. Based on reinforcement learning and sampling and through a loss function, their proposed model learned

to generate captions for the given image. According to [37], existing image captioning models are trained via maximum likelihood estimation. However, a limitation is that the log-likelihood score of some descriptions cannot well correlated with human assessments of quality. In [12], a deliberate residual attention image captioning model was proposed. In the proposed model, the layer of first-pass residual-based attention was used to generate hidden states and visual attention. A preliminary image description was then created. The layer of second-pass deliberate residual-based attention was used to refine the preliminary image description. As stated in [12], the second-pass is based on global features captured by the visual attention and hidden layer in the first-pass. Hence, their proposed approach has the potential to generate a better image caption. In [45], the authors proposed a unified attention block that fully employs bilinear pooling to perform reasoning or selectively capitalize on visual information. Existing conventional medical image captioning methods, e.g., [27, 31, 34], are mainly based on traditional natural image captioning approaches. A limitation of traditional image captioning methods is that although these models work well on natural image captioning datasets, they do not generalize well to medical image captioning datasets. An image captioning model reinforced by context, e.g., keywords, is a more promising way to generate a better description for a medical image [26]. In this work, a new context-driven model is introduced to improve the performance of the medical image captioning model.

2.2 Multi-modal Medical Image Captioning

Recently, a multi-modal task visual question answering (VQA) has been introduced [18–22, 39–41]. The goal of VQA is to output a text-based answer for an input text-based question with a given image. Since a VQA model has textual and visual inputs, one modality is used to help the other [2]. A similar idea of multiple input modalities can be also applied to build a multi-modal related [27] or a multi-modal medical image captioning model [26]. The authors of [27] proposed a multi-modal related method to generate a medical description for a given lung X-ray image. Their proposed approach only has an image input modality and the image input is used to generate intermediate/side products, i.e., text-based tags, to reinforce the later generation of a medical description. However, the model-generated intermediate products could be wrong/bias information and it could confuse models during the training phase. Hence, in [26], a model with multi-modal inputs, i.e., a set of expert-defined keywords and a retina image, was introduced to generate a better quality of medical description. The expert-defined keywords help models learn better because the correctness/quality of the keywords is guaranteed by experts [26]. Although considering expert-defined keywords as one of the multi-modal inputs could improve the model performance, effective textual input encoding will become another challenge. In this work, a new model with an effective textual input embedding method is introduced to tackle this challenge.

2.3 Word Embeddings

In this work, word embedding methods are categorized into three categories, i.e., the BoW, static word embeddings, and contextualized word representations.

Bag of Words. BoW model [13] is a simplifying representation commonly used in information retrieval, NLP, and computer vision. In BoW, a sentence/document is represented as the bag of its words which keeps word multiplicity. The frequency of each word is used as a feature for training a model. According to [26, 52, 55], since the BoW method likely cannot capture semantic meaning effectively, the method is not effective enough in multi-modal medical image captioning.

Static Word Embeddings. As stated in [9], Skip-gram with negative sampling (SGNS) [42] and GloVe [47] are among the best-known models for generating static word embeddings. In practice, these models learn word embeddings iteratively, but it has been proven that the models both implicitly factorize a word-context matrix containing a co-occurrence statistic [32, 33]. A notable issue with the static word embeddings is that all senses of a polysemous word must share a single vector because a single representation for each word is created.

Contextualized Word Representations. To tackle the above issue, the authors of [8, 48, 50] have proposed various deep neural language models to create context-sensitive word representations. The models are fine-tuned to create deep learning-based models for a wide range of downstream NLP tasks. In these models, the internal representations of words are considered as a function of the entire textual input. Hence, the representations are called contextualized word representations. In [36], an approach was introduced suggesting that these representations capture task-agnostic and highly transferable properties of language. The authors of [48] introduced a method to generate contextualized representations of every token by concatenating the internal states of a 2-layer bi-LSTM. In [50], the proposed approach is an uni-directional transformer-based language model [57]. The method introduced in [8] is a bi-directional transformer-based language model [57]. According to [9], the method of contextualized word representations is more effective than the static word embeddings. Hence, in this work, we propose to base on the contextualized word representations to develop a new model for multi-modal medical image captioning.

2.4 Retinal Image Dataset

Recently, various medical image datasets have been proposed for research, e.g., retinal image datasets [1, 3, 5–7, 11, 15–17, 23–26, 29, 38, 43, 44, 49, 54, 56, 58, 61, 62]. The above related existing retinal image datasets are reviewed in this subsection.

In [16], the proposed dataset STARE contains 397 images and it is used to develop an automatic system for diagnosing human eye diseases. The authors of [56] proposed a dataset DRIVE with 40 retina images, half for the training set and the other half for the testing set. For the training, a single manual segmentation of the vasculature is available. For the testing, two manual segmentations are available. In [29], the proposed dataset DIARETDB1 consists of 89 color fundus images. 84 images of them contain at least mild non-proliferative signs of Diabetic Retinopathy (DR). The remaining five images are considered normal without containing any signs of DR. In [3], the proposed dataset REVIEW with 14 images is designed for a segmentation task. The proposed dataset DRIONS-DB in [5] contains 110 colorful retinal images. The proposed dataset

contains several visual characteristics, e.g., cataract (severe or moderate), light artifacts, some of the rim blurred or missing, concentric peripapillary atrophy/artifacts, moderate peripapillary atrophy, and strong pallor distractor. The retinal image dataset VARIA [44] is used for authentication purposes. It contains 233 images from 139 different individuals. The proposed dataset INSPIRE-AVR in [43] consists of 40 colorful retinal images of the vessels and optic disc and an arterio-venous ratio reference standard. The authors of [6] proposed a dataset ONHSD with 99 retinal images for a segmentation task. In [11], the introduced dataset CHASE-DB1 with 14 retinal images is used for retinal vessel analysis. The dataset VICAVR [58] for the computation of the ratio of Artery/Vein (A/V) consists of 58 retinal images. The proposed dataset Drishti-GS in [54] has 101 images, 50 for training and 51 for testing. The MESSIDOR dataset [7] has 1,200 colorful eye fundus images without manual annotation, e.g., lesions contours or position. The RODREP dataset [1] consists of repeated 1,120 4-field colorful fundus images of 70 patients in the DR screening program of the Rotterdam Eye Hospital. In [15], the proposed dataset FIRE contains 129 retinal images, forming 134 image pairs. The image pairs are split into three different categories depending on their characteristics. The authors of [49] proposed a dataset IDRiD containing 516 retinal fundus images. In the proposed dataset, the ground truths associated with the signs of DR, Diabetic Macular Edema (DME), and normal retinal structures are given as follows: (i) Pixel level labels of typical DR lesions and optic disc; (ii) Optic disc and fovea center coordinates; (iii) Image level disease severity grading of DR and DME. Although there are many existing retinal image datasets, not each of them is tailored for multi-modal retinal image captioning. Since the dataset introduced by [26] is large-scale and specially designed for multi-modal deep learning research, in this work, the experiments are mainly based on [26]’s DeepEyeNet (DEN) dataset.

3 METHODOLOGY

In this section, the proposed multi-modal medical image captioning model is described in detail. The proposed method consists of a contextualized keyword encoder and a medical description generator. Flowchart of the proposed model is presented in Figure 2.

3.1 Contextualized Keyword Encoder

Transformer consists of a transformer-encoder and a transformer-decoder [57]. Transformer architecture has been used with success in language modeling and machine translation. The transformer-encoder and transformer-decoder are the stacks of multiple basic transformer blocks. The proposed model is inspired by the GPT-2 structure, i.e., a transformer-decoder-like structure, in terms of its parallelization and masked self-attention. Its characteristics are deployed to develop the proposed contextualized keyword encoder for the embedding of keywords. Detail of the contextualized keyword encoder is presented as follows:

$$x_n = W_e * k_n, n \in \{0, \dots, N - 1\}, \quad (1)$$

where x_n is an input token/keyword embedding, $W_e \in \mathbb{R}^{E_s \times V_s}$ indicates the token embedding matrix, E_s denotes the word embedding size, V_s indicates the vocabulary size, k_n denotes an input token/keyword, and N denotes the number of input tokens/keywords.

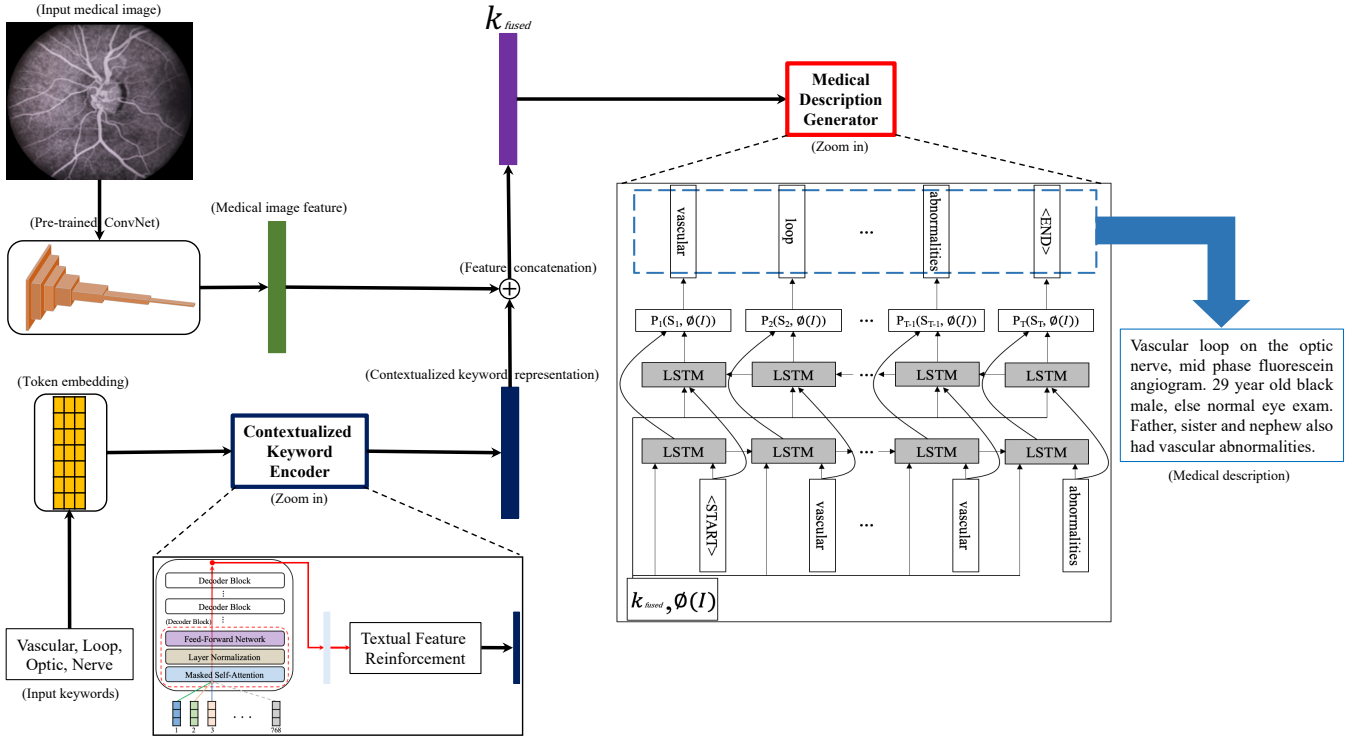


Figure 2: Flowchart of proposed multi-modal medical image captioning model. A pre-trained CNN, e.g., VGG16 or VGG19 pre-trained on ImageNet, is used to extract features from the medical image input (dark green). From a set of input keywords, the “Token embedding” generates the input to the “Contextualized Keyword Encoder” which is composed of a stack of decoder blocks and “Textual Feature Reinforcement”. Each decoder block consists of the masked self-attention, layer normalization, and feed-forward network (red dashed line box). “Textual Feature Reinforcement”, i.e., a stack of fully-connected layers, generates the contextualized keyword representation (dark blue). Note that 768 color-coded brick-stacked vectors are the input of the keyword encoder. \oplus indicates the concatenation of the medical image feature and contextualized keyword representation. In “Medical Description Generator” which creates the medical description, k_{fused} denotes a fused feature vector (purple), $\phi(I)$ denotes an image feature vector, and $P_i(S_i, \phi(I))$ is a probability distribution where $i = 1, 2, \dots, T$. See the *Methodology* section for more details.

Masked Self-attention Mechanism. The mechanism of masked self-attention is described as follows:

$$Q = W_q * x_n + b_q, \quad (2)$$

where Q denotes the representation of the current word [57]. One linear layer, i.e., $W_q \in \mathbb{R}^{H_s \times E_s}$ with bias term b_q and output size H_s , is used to generate Q .

$$K = W_k * x_n + b_k, \quad (3)$$

where K is the key vector [57]. One linear layer, i.e., $W_k \in \mathbb{R}^{H_s \times E_s}$ with bias term b_k and output size H_s , is used to generate K .

$$V = W_v * x_n + b_v, \quad (4)$$

where V denotes the value vector [57]. One linear layer, i.e., $W_v \in \mathbb{R}^{H_s \times E_s}$ with bias term b_v and output size H_s , is used to generate V .

$$MaskAtten(Q, K, V) = softmax(m(\frac{QK^T}{\sqrt{d_k}}))V, \quad (5)$$

where $m(\cdot)$ is a masked self-attention function and d_k denotes a scaling factor [57].

Layer Normalization. The layer normalization is calculated as Equation-(6).

$$Z_{Norm} = LayerNorm(MaskAtten(Q, K, V)), \quad (6)$$

where $LayerNorm(\cdot)$ is a function for layer normalization and $MaskAtten(Q, K, V)$ is the result from Equation-(5).

Contextualized Keyword Representation. Through the above, i.e., Equation-(1), Equation-(2), Equation-(3), Equation-(4), Equation-(5), and Equation-(6), the contextualized keyword representation F is derived as:

$$F = FFN(Z_{Norm}) = \sigma(W_1 Z_{Norm} + b_1)W_2 + b_2, \quad (7)$$

where $FFN(\cdot)$ denotes a position-wise feed-forward network (FFN), σ indicates an activation function. W_1 , W_2 , b_1 , and b_2 are learnable parameters of the FFN. Note that in practice, a stack of fully-connected layers is used to reinforce F , referring to Figure 2.

3.2 Loss Function

In this work, medical description generation is modeled as a classification problem. Hence, the categorical cross-entropy loss function

is adopted to build the proposed method, referring to Equation-(8).

$$Loss = -\frac{1}{N} \sum_{i=0}^{N-1} \sum_{c=0}^{C-1} \mathbf{1}_{y_i \in C_c} \log(P_{model}[y_i \in C_c]), \quad (8)$$

where N denotes the number of observations, C indicates the number of categories, $\mathbf{1}_{y_i \in C_c}$ denotes an indicator function of the i -th observation belonging to the c -th category, and $P_{model}[y_i \in C_c]$ is the probability predicted by the model for the i -th observation to belong to the c -th category.

When there are more than two categories, the neural network model outputs a probability vector with C dimensions. Each element in the vector gives the probability that the model input should be classified as belonging to the respective category. Note that when the number of categories is two, the categorical cross-entropy loss degenerates to the binary cross-entropy loss, i.e., a special case of the categorical cross-entropy loss. In this case, the neural network outputs a single probability \hat{y}_i , with the other one being $1 - \hat{y}_i$.

3.3 Medical Description Generator

For the medical description generator, the CNN medical image encoder ϕ used in [26] is adopted to extract the image feature. The extracted feature is fed in each time step of a subsequent bidirectional LSTM model. $p(S_t|I, S_0, \dots, S_{t-1})$ denotes all of the preceding words, and $S = (S_0, \dots, S_T)$ indicates a true sentence describing the input image I .

The medical description generator is unrolled as follows:

$$e_t = W_d \times \phi(I), t \in \{0, \dots, T\}, \quad (9)$$

where $W_d \in \mathbb{R}^{E \times F}$ denotes a fully-connected layer, E represents the word embedding size, and F is the image feature size.

$$x_t = W_e S_t, t \in \{0, \dots, T\}, \quad (10)$$

where each word is represented as a bag-of-words id S_t , and the sentence S and the image I are mapped to the same high dimensional space.

$$P_t = BiLSTM([e_t, k_{fused}, x_t]), t \in \{0, \dots, T\}, \quad (11)$$

where in Equation-(11), for each time step, image contents e_t , fused multi-modal feature k_{fused} , and ground truth word vector x_t are fed to the network to strengthen its memory of images.

4 EXPERIMENTS AND ANALYSIS

In this section, the dataset and evaluation metrics used in the experiments are introduced and the experimental setup is described in detail. Then, the effectiveness of the proposed multi-modal medical image captioning model is analyzed. Finally, several randomly selected qualitative results are displayed.

4.1 Dataset and Evaluation Metrics

Dataset. In [26], a state-of-the-art model and a large-scale retinal image dataset with unique expert-defined keyword annotations are introduced for multi-modal medical image captioning. The dataset is composed of 1,811 grey-scale Fluorescein Angiography (FA) images and 13,898 colorful Color Fundus Photography (CFP) images. Each image in the dataset has two corresponding labels, i.e., the clinical description and expert-defined keywords. In [26]’s proposed dataset, the longest word length is more than 15 words and 50 words

for keywords and clinical descriptions, respectively. The average word length of the keywords and clinical descriptions is between 5 words and 10 words. The dataset contains 265 different retinal diseases/symptoms including the common and non-common. According to [26], the expert-defined keywords are collected from the ophthalmologists’ or retinal specialists’ retinal image analysis and diagnosis records with patients. Hence, the keywords contain information about potential retinal diseases, retinal symptoms, or patients’ characteristics. In [26], the entire dataset is divided into 60%/20%/20% for training/validation/testing, respectively.

Evaluation Metrics. The same medical description evaluation metrics used in [26] are adopted in this work to quantify the performance of the proposed model, i.e., BLEU [46], CIDEr [59], and ROUGE [35]. Another commonly used text evaluation metric METEOR [4] is also used to evaluate the proposed method. The aforementioned evaluation metrics are defined as follows:

$$BP = \begin{cases} 1 & \text{if } c > r \\ \exp(1 - \frac{r}{c}) & \text{if } c \leq r \end{cases}; BLEU = BP \cdot \exp\left(\sum_{n=1}^N w_n \log p_n\right), \quad (12)$$

where r denotes the effective ground truth text length, c indicates the length of the prediction text, and BP denotes brevity penalty. The geometric average of the modified n -gram precisions p_n is computed by using n -grams up to length N and positive weights w_n summing to 1.

$$CIDEr_n(c_i, S_i) = \frac{1}{m} \sum_j \frac{g^n(c_i) \cdot g^n(s_{ij})}{\|g^n(c_i)\| \|g^n(s_{ij})\|}; \quad (13)$$

$$CIDEr(c_i, S_i) = \sum_{n=1}^N w_n CIDEr_n(c_i, S_i),$$

where c_i denotes prediction text, $S_i = \{s_{i1}, \dots, s_{im}\}$ denotes a set of ground truth descriptions. $CIDEr_n(c_i, S_i)$ score for n -grams of length n is computed by using the average cosine similarity between c_i and S_i , which accounts for both precision and recall. $g^n(c_i)$ is a vector formed by $g_k(c_i)$ corresponding to all n -grams of length n , and $\|g^n(c_i)\|$ denotes the magnitude of $g^n(c_i)$. Similarly for $g^n(s_{ij})$. The higher order (longer) n -grams is used to capture grammatical properties as well as richer semantics. $CIDEr(c_i, S_i)$ indicated the combined score based on n -grams of varying lengths.

$$R_{lcs} = \frac{LCS(X, Y)}{m}; P_{lcs} = \frac{LCS(X, Y)}{n}; F_{lcs} = \frac{(1 + \beta^2)R_{lcs}P_{lcs}}{R_{lcs} + \beta^2P_{lcs}}, \quad (14)$$

where the longest common subsequence (LCS) based F-measure $F_{lcs}/ROUGE-L$ is used to estimate the similarity between ground truth text $X = \{x_1, \dots, x_m\}$ with length m and prediction text $Y = \{y_1, \dots, y_n\}$ with length n . β is to balance the relative importance between P_{lcs} and R_{lcs} .

$$METEOR_{score} = \frac{10PR}{R + 9P} \left(1 - 0.5 \left(\frac{\#chunks}{\#unigrams_matched}\right)^3\right), \quad (15)$$

where P denotes unigram precision, R denotes unigram recall, $\#chunks$ indicates number of chunks, and $\#unigrams_matched$ denotes number of matched unigrams, referring to [4] for detail.

Table 1: Comparison with the state-of-the-art “DeepOpht with BoW” [26], based on the metric of BLEU [46], CIDEr [59], ROUGE [35], and METEOR [4]. Proposed method outperforms the model in [26] by +53.2% in BLEU-avg and +18.6% in CIDEr. The results are based on VGG16 image feature extractor pre-trained on ImageNet and beam search algorithm in the testing phase. Note that BLEU-avg indicates the average score of BLEU-1, BLEU-2, BLEU-3, and BLEU-4. “beam” denotes number of beams used in the beam search. * denotes not available. Similar notations also used in Table 2. In general, the proposed method already beats baseline with beam=1, i.e., no beam search used, in BLEU and CIDEr and competitive in ROUGE-L.

Model	BLEU-1	BLEU-2	BLEU-3	BLEU-4	BLEU-avg	CIDEr	ROUGE-L	METEOR
DeepOpht with BoW (beam=3) [26]	0.144	0.092	0.052	0.021	0.077	0.296	0.197	*
Proposed Model with GloVe (beam=1)	0.173	0.111	0.072	0.048	0.101	0.243	0.164	0.153
Proposed Model with GPT-2 (beam=1)	0.192	0.130	0.088	0.060	0.118	0.351	0.188	0.167

Table 2: Comparison with the state-of-the-art “DeepOpht with BoW” [26]. The results are based on VGG19 image feature extractor pre-trained on ImageNet and beam search algorithm in the testing phase. Proposed method outperforms the model in [26] by +30% in BLEU-avg and +8% in CIDEr.

Model	BLEU-1	BLEU-2	BLEU-3	BLEU-4	BLEU-avg	CIDEr	ROUGE-L	METEOR
DeepOpht with BoW (beam=3) [26]	0.184	0.114	0.068	0.032	0.100	0.361	0.232	*
Proposed Model with GloVe (beam=1)	0.192	0.132	0.093	0.067	0.121	0.356	0.186	0.169
Proposed Model with GloVe (beam=3)	0.201	0.139	0.098	0.071	0.127	0.359	0.203	0.184
Proposed Model with GPT-2 (beam=1)	0.203	0.137	0.093	0.065	0.125	0.356	0.197	0.174
Proposed Model with GPT-2 (beam=3)	0.203	0.142	0.100	0.073	0.130	0.389	0.211	0.188

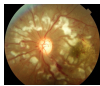
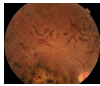
Input Retinal Image	Expert-defined Input Keywords	Ground Truth Caption	Generated Description by Proposed Method
	Hypertensive, retinopathy	2 months post htn tx.	Bilateral hypertensive retinopathy in a 19 year old girl with renal disease, hypertension and anemia.
	Color, fundus, photograph, bilateral, pigmentary, retinopathy, macular, coloboma	Color fundus photograph of the right eye of a 25-year-old woman with the history of low vision since childhood. bilateral macular colobomata and pigmentary retinopathy similar to leber's congenital amaurosis are present.	Color fundus photograph of the right eye of a 24 year old woman with leber's congenital amaurosis.

Figure 3: Randomly selected qualitative results of the proposed multi-modal medical image captioning. The result shows that the proposed model exploits the effective contextualized keyword representations as guidance to generate meaningful medical descriptions. Note that in practice, “date”, “skin color”, “gender”, and “age” would be part of the dataset and that a system should make it part of the medical description by slot filling or post-processing [26].

4.2 Experimental Setup

Similar to [26], in this work, VGG16 and VGG19 pre-trained on ImageNet are adopted to extract image features. To process keywords and descriptions, non-alphabet characters are removed, all remaining characters are converted to lower-case, and all the words appearing only once are replaced by a special token $\langle UNK \rangle$. When keywords are excluded, the vocabulary size is 4,007. When keywords are included, the vocabulary size is 4,292. All sentences are truncated or padded with a maximum length of 50. A token/word embedding size 300 is used to encode every word. Since the proposed contextualized keyword encoder is based on the GPT-2 architecture [50], using the pre-trained weight of GPT-2 for initialization is helpful in the experiments. As stated in [50], GPT-2 has been pre-trained on a large corpus with vocabulary size 50,257. For the proposed medical description generator, a hidden layer size 256 is used for the LSTM unit. The default setup of [26]’s dataset is used for experiments, i.e., 60%/20%/20% for training/validation/testing, respectively. In this work, Keras is used for implementation, and models are trained with

2 epochs, 64 batch size, $1e-3$ learning rate, and Adam optimizer [30]. For the hyperparameters of Adam optimizer, coefficients used for computing moving averages of gradient and its square are $\beta_1 = 0.9$ and $\beta_2 = 0.999$, respectively. $\epsilon = 1e-8$ is added to the denominator to improve numerical stability.

4.3 Effectiveness Analysis

According to Table 1 and Table 2, the results show that the proposed model with contextualized keyword representations and static word embeddings beat the baseline model with BoW [26]. Moreover, the model with contextualized keyword representations outperforms the model with static word embeddings [47]. Since contextualized keyword representations effectively capture the keywords information, the performance of the multi-modal medical image captioning model is improved, +53.2% in BLEU-avg and +18.6% in CIDEr, and a better quality of medical description is generated. Note that although the beam search algorithm with three beams boosts model performance in the testing phase, the computational cost is around 12 times of with one beam (14851/1265 in seconds). Qualitative results are demonstrated in Figure 3.

5 CONCLUSION

To sum up, in this paper a new end-to-end deep model is introduced for multi-modal medical image captioning. The contextualized keyword representation, textual feature reinforcement module, and masked self-attention are used to develop the proposed method. The effectiveness of the proposed model is thoroughly evaluated through experiments on the existing multi-modal retinal image captioning dataset proposed by [26]. The experimental results show that the proposed method outperforms the baseline model. The model performance is increased in terms of BLEU and CIDEr.

ACKNOWLEDGMENTS

This work is supported by competitive research funding from the University of Amsterdam.

REFERENCES

- [1] Kedir M Adal, Peter G van Etten, Jose P Martinez, Lucas J van Vliet, and Koenraad A Vermeer. 2015. Accuracy assessment of intra-and intervisit fundus image registration for diabetic retinopathy screening. *Investigative ophthalmology & visual science* 56, 3 (2015), 1805–1812.
- [2] Aishwarya Agrawal, Jiasen Lu, Stanislaw Antol, Margaret Mitchell, C Lawrence Zitnick, Devi Parikh, and Dhruv Batra. 2017. Vqa: Visual question answering. *International Journal of Computer Vision* 123, 1 (2017), 4–31.
- [3] Bashir Al-Diri, Andrew Hunter, David Steel, Maged Habib, Taghreed Hudaib, and Simon Berry. 2008. A reference data set for retinal vessel profiles. In *2008 30th Annual International Conference of the IEEE Engineering in Medicine and Biology Society*. IEEE, 2262–2265.
- [4] Satanjeev Banerjee and Alon Lavie. 2005. METEOR: An automatic metric for MT evaluation with improved correlation with human judgments. In *Proceedings of the acl workshop on intrinsic and extrinsic evaluation measures for machine translation and/or summarization*. 65–72.
- [5] Enrique J Carmona, Mariano Rincón, Julián García-Feijóo, and José M Martínez-de-la Casa. 2008. Identification of the optic nerve head with genetic algorithms. *Artificial Intelligence in Medicine* 43, 3 (2008), 243–259.
- [6] Retinal Image Computing. 2012. Understanding, “ONHSD-Optic Nerve Head Segmentation Dataset,” University of Lincoln, United Kingdom, 2004.
- [7] Etienne Decencière, Xiwei Zhang, Guy Cazuguel, Bruno Lay, Béatrice Cochener, Caroline Trone, Philippe Gain, Richard Ordonez, Pascale Massin, Ali Erginay, et al. 2014. Feedback on a publicly distributed image database: the Messidor database. *Image Analysis & Stereology* 33, 3 (2014), 231–234.
- [8] Jacob Devlin, Ming-Wei Chang, Kenton Lee, and Kristina Toutanova. 2018. Bert: Pre-training of deep bidirectional transformers for language understanding. *arXiv preprint arXiv:1810.04805* (2018).
- [9] Kavin Ethayarajah. 2019. How contextual are contextualized word representations? comparing the geometry of BERT, ELMo, and GPT-2 embeddings. *arXiv preprint arXiv:1909.00512* (2019).
- [10] Hao Fang, Saurabh Gupta, Forrest Iandola, Rupesh K Srivastava, Li Deng, Piotr Dollár, Jianfeng Gao, Xiaocong He, Margaret Mitchell, John C Platt, et al. 2015. From captions to visual concepts and back. In *Proceedings of the IEEE conference on computer vision and pattern recognition*. 1473–1482.
- [11] Muhammad Moazam Fraz, Paolo Remagnino, Andreas Hoppe, Bunyarit Uyyanonvara, Alicja R Rudnicka, Christopher G Owen, and Sarah A Barman. 2012. An ensemble classification-based approach applied to retinal blood vessel segmentation. *IEEE Transactions on Biomedical Engineering* 59, 9 (2012), 2538–2548.
- [12] Lianli Gao, Kaixuan Fan, Jingkuan Song, Xianglong Liu, Xing Xu, and Heng Tao Shen. 2019. Deliberate Attention Networks for Image Captioning. *AAAI* (2019).
- [13] Zellig S Harris. 1954. Distributional structure. *Word* 10, 2-3 (1954), 146–162.
- [14] Lisa Anne Hendricks, Zeynep Akata, Marcus Rohrbach, Jeff Donahue, Bernt Schiele, and Trevor Darrell. 2016. Generating visual explanations. In *European Conference on Computer Vision*. Springer, 3–19.
- [15] Carlos Hernandez-Matas, Xenophon Zabulis, Areti Triantafyllou, Panagiota Anyfanti, Stella Douma, and Antonis A Argyros. 2017. FIRE: fundus image registration dataset. *Journal for Modeling in Ophthalmology* 1, 4 (2017), 16–28.
- [16] Adam Hoover and Michael Goldbaum. 2003. Locating the optic nerve in a retinal image using the fuzzy convergence of the blood vessels. *IEEE transactions on medical imaging* 22, 8 (2003), 951–958.
- [17] Tao Hu, Pascal Mettes, Jia-Hong Huang, and Cees GM Snoek. 2019. Silco: Show a few images, localize the common object. In *Proceedings of the IEEE/CVF International Conference on Computer Vision*. 5067–5076.
- [18] Jia-Hong Huang. 2017. Robustness Analysis of Visual Question Answering Models by Basic Questions. *King Abdullah University of Science and Technology MS thesis* (2017).
- [19] Jia-Hong Huang, Modar Alfadly, and Bernard Ghanem. 2017. Vqabq: Visual question answering by basic questions. *CVPR VQA Challenge Workshop* (2017).
- [20] Jia-Hong Huang, Modar Alfadly, Bernard Ghanem, and Marcel Worring. 2019. Assessing the robustness of visual question answering. *arXiv preprint arXiv:1912.01452* (2019).
- [21] Jia-Hong Huang, Cuong Duc Dao, Modar Alfadly, and Bernard Ghanem. 2019. A novel framework for robustness analysis of visual qa models. In *Proceedings of the AAAI Conference on Artificial Intelligence*, Vol. 33. 8449–8456.
- [22] Jia-Hong Huang, Cuong Duc Dao, Modar Alfadly, C Huck Yang, and Bernard Ghanem. 2018. Robustness analysis of visual qa models by basic questions. *CVPR VQA Challenge and Visual Dialog Workshop* (2018).
- [23] Jia-Hong Huang, Luka Murn, Marta Mrak, and Marcel Worring. 2021. GPT2MVS: Generative Pre-trained Transformer-2 for Multi-modal Video Summarization. In *Proceedings of the 2021 International Conference on Multimedia Retrieval*. 242–250.
- [24] Jia-Hong Huang and Marcel Worring. 2020. Query-controllable video summarization. In *Proceedings of the 2020 International Conference on Multimedia Retrieval*. 242–250.
- [25] Jia-Hong Huang, Ting-Wei Wu, Chao-Han Huck Yang, and Marcel Worring. 2021. Deep Context-Encoding Network for Retinal Image Captioning. *arXiv preprint arXiv*.
- [26] Jia-Hong Huang, C-H Huck Yang, Fangyu Liu, Meng Tian, Yi-Chieh Liu, Ting-Wei Wu, I Lin, Kang Wang, Hiromasa Morikawa, Henghua Chang, et al. 2021. DeepOph: medical report generation for retinal images via deep models and visual explanation. In *Proceedings of the IEEE/CVF winter conference on applications of computer vision*. 2442–2452.
- [27] Baoyu Jing, Pengtao Xie, Eric Xing, Baoyu Jing, Pengtao Xie, and Eric Xing. 2018. On the automatic generation of medical imaging reports. *ACL* (2018).
- [28] Andrej Karpathy and Li Fei-Fei. 2015. Deep visual-semantic alignments for generating image descriptions. In *CVPR*. 3128–3137.
- [29] Tomi Kauppi, Valentina Kalesnykiene, Joni-Kristian Kamarainen, Lasse Lensu, Iris Sorri, A Raninen, R Voutilainen, J Pietilä, H Kälviäinen, and H Uusitalo. 2007. DIARETDB1—Standard Diabetic Retinopathy Database Calibration level 1.
- [30] Diederik P Kingma and Jimmy Ba. 2014. Adam: A method for stochastic optimization. *arXiv preprint arXiv:1412.6980* (2014).
- [31] Jonathan Laserson, Christine Dan Lantsman, Michal Cohen-Sfady, Itamar Tamir, Eli Goz, Chen Brestel, Shir Bar, Maya Atar, and Eldad Elnekave. 2018. Text-tray: Mining clinical reports to gain a broad understanding of chest x-rays. In *International Conference on Medical Image Computing and Computer-Assisted Intervention*. Springer, 553–561.
- [32] Omer Levy and Yoav Goldberg. 2014. Linguistic regularities in sparse and explicit word representations. In *Proceedings of the eighteenth conference on computational natural language learning*. 171–180.
- [33] Omer Levy and Yoav Goldberg. 2014. Neural word embedding as implicit matrix factorization. *NIPS* 27 (2014), 2177–2185.
- [34] Yuan Li, Xiaodan Liang, Zhiting Hu, and Eric P Xing. 2018. Hybrid retrieval-generation reinforced agent for medical image report generation. In *Advances in Neural Information Processing Systems*. 1530–1540.
- [35] Chin-Yew Lin. 2004. Rouge: A package for automatic evaluation of summaries. *Text Summarization Branches Out* (2004).
- [36] Nelson F Liu, Matt Gardner, Yonatan Belinkov, Matthew E Peters, and Noah A Smith. 2019. Linguistic knowledge and transferability of contextual representations. *arXiv preprint arXiv:1903.08855* (2019).
- [37] Siqi Liu, Zhenhai Zhu, Ning Ye, Sergio Guadarrama, and Kevin Murphy. 2017. Improved image captioning via policy gradient optimization of spider. In *Proceedings of the IEEE international conference on computer vision*. 873–881.
- [38] Yi-Chieh Liu, Hao-Hsiang Yang, C-H Huck Yang, Jia-Hong Huang, Meng Tian, Hiromasa Morikawa, Yi-Chang Hsueh, Kai Chen, and Jesper Tegner. 2018. Synthesizing new retinal symptom images by multiple generative models. In *Asian Conference on Computer Vision*. Springer, 235–250.
- [39] Mateusz Malinowski and Mario Fritz. 2014. A multi-world approach to question answering about real-world scenes based on uncertain input. *arXiv preprint arXiv:1410.0210* (2014).
- [40] Mateusz Malinowski, Marcus Rohrbach, and Mario Fritz. 2015. Ask your neurons: A neural-based approach to answering questions about images. In *Proceedings of the IEEE international conference on computer vision*. 1–9.
- [41] Mateusz Malinowski, Marcus Rohrbach, and Mario Fritz. 2017. Ask your neurons: A deep learning approach to visual question answering. *International Journal of Computer Vision* 125, 1 (2017), 110–135.
- [42] Tomas Mikolov, Ilya Sutskever, Kai Chen, Greg Corrado, and Jeffrey Dean. 2013. Distributed representations of words and phrases and their compositionality. *arXiv preprint arXiv:1310.4546* (2013).
- [43] M Niemeijer, X Xu, A Dumitrescu, P Gupta, B van Ginneken, J Folk, and M Abramoff. 2011. INSPIRE-AVR: Iowa normative set for processing images of the retina-artery vein ratio.
- [44] Marcos Ortega, Manuel G Penedo, José Rouco, Noelia Barreira, and María J Carreira. 2009. Retinal verification using a feature points-based biometric pattern. *EURASIP Journal on Advances in Signal Processing* 2009 (2009), 2.
- [45] Yingwei Pan, Ting Yao, Yehao Li, and Tao Mei. 2020. X-Linear Attention Networks for Image Captioning. In *Proceedings of the IEEE/CVF Conference on Computer Vision and Pattern Recognition*. 10971–10980.
- [46] Kishore Papineni, Salim Roukos, Todd Ward, and Wei-Jing Zhu. 2002. BLEU: a method for automatic evaluation of machine translation. In *Proceedings of ACL*. Association for Computational Linguistics, 311–318.
- [47] Jeffrey Pennington, Richard Socher, and Christopher D Manning. 2014. Glove: Global vectors for word representation. In *Proceedings of the 2014 conference on empirical methods in natural language processing (EMNLP)*. 1532–1543.
- [48] Matthew E Peters, Mark Neumann, Mohit Iyyer, Matt Gardner, Christopher Clark, Kenton Lee, and Luke Zettlemoyer. 2018. Deep contextualized word representations. *arXiv preprint arXiv:1802.05365* (2018).
- [49] Prasanna Porwal, Samiksha Pachade, Ravi Kamble, Manesh Kokare, Girish Deshmukh, Vivek Sahasrabudde, and Fabrice Meriaudeau. 2018. Indian diabetic retinopathy image dataset (IDRiD): a database for diabetic retinopathy screening research. *Data* 3, 3 (2018), 25.
- [50] Alec Radford, Jeffrey Wu, Rewon Child, David Luan, Dario Amodei, and Ilya Sutskever. 2019. Language models are unsupervised multitask learners. *OpenAI blog* 1, 8 (2019), 9.

- [51] Olga Russakovsky, Jia Deng, Hao Su, Jonathan Krause, Sanjeev Satheesh, Sean Ma, Zhiheng Huang, Andrej Karpathy, Aditya Khosla, Michael Bernstein, et al. 2015. Imagenet large scale visual recognition challenge. *International journal of computer vision* 115, 3 (2015), 211–252.
- [52] Sam Scott and Stan Matwin. 1998. Text classification using WordNet hypernyms. In *Usage of WordNet in Natural Language Processing Systems*.
- [53] Karen Simonyan and Andrew Zisserman. 2014. Very deep convolutional networks for large-scale image recognition. *arXiv preprint arXiv:1409.1556* (2014).
- [54] Jayanthi Sivaswamy, SR Krishnadas, Gopal Datt Joshi, Madhulika Jain, and A Ujjwaft Syed Tabish. 2014. Drishti-gs: Retinal image dataset for optic nerve head (onh) segmentation. In *2014 IEEE 11th International Symposium on Biomedical Imaging (ISBI)*. IEEE, 53–56.
- [55] K Soumya George and Shibly Joseph. 2014. Text classification by augmenting bag of words (BOW) representation with co-occurrence feature. *IOSR J. Comput. Eng* 16, 1 (2014), 34–38.
- [56] Joes Staal, Michael D Abràmoff, Meindert Niemeijer, Max A Viergever, and Bram Van Ginneken. 2004. Ridge-based vessel segmentation in color images of the retina. *TMI* 23, 4 (2004), 501–509.
- [57] Ashish Vaswani, Noam Shazeer, Niki Parmar, Jakob Uszkoreit, Llion Jones, Aidan N Gomez, Lukasz Kaiser, and Illia Polosukhin. 2017. Attention is all you need. *arXiv preprint arXiv:1706.03762* (2017).
- [58] SG Vázquez, Brais Cancela, Noelia Barreira, Manuel G Penedo, M Rodríguez-Blanco, M Pena Seijo, G Coll de Tuero, Maria Antònia Barceló, and Marc Saez. 2013. Improving retinal artery and vein classification by means of a minimal path approach. *Machine vision and applications* 24, 5 (2013), 919–930.
- [59] Ramakrishna Vedantam, C Lawrence Zitnick, and Devi Parikh. 2015. Cider: Consensus-based image description evaluation. In *Proceedings of the IEEE conference on computer vision and pattern recognition*. 4566–4575.
- [60] Oriol Vinyals, Alexander Toshev, Samy Bengio, and Dumitru Erhan. 2015. Show and tell: A neural image caption generator. In *2015 IEEE Computer Society Conference on Computer Vision and Pattern Recognition (CVPR'15)*. 3156–3164.
- [61] C-H Huck Yang, Jia-Hong Huang, Fangyu Liu, Fang-Yi Chiu, Mengya Gao, Weifeng Lyu, Jesper Tegner, et al. 2018. A novel hybrid machine learning model for auto-classification of retinal diseases. *ICML Workshop on Computational Biology* (2018).
- [62] C-H Huck Yang, Fangyu Liu, Jia-Hong Huang, Meng Tian, MD I-Hung Lin, Yi Chieh Liu, Hiromasa Morikawa, Hao-Hsiang Yang, and Jesper Tegner. 2018. Auto-classification of retinal diseases in the limit of sparse data using a two-streams machine learning model. In *Asian Conference on Computer Vision*. Springer, 323–338.